Beretta et al.; **Immunohistochemical and Morphometric Evaluation of Gastrocnemius Muscle and Myotendinous Junction of Golden Retriever Dogs with Muscular Dystrophy**. Braz J Vet Pathol, 2014, 7(2), 70 - 81

70

Original Full Paper

Immunohistochemical and Morphometric Evaluation of Gastrocnemius Muscle and Myotendinous Junction of Golden Retriever Dogs with Muscular Dystrophy

Daniel Côrtes Beretta[1], Julieta Rodini Engracia Moraes [2]*, Jair Rodini Engracia Filho[2],
Lygia Maria Mouri Malvestio[2], Flávio Ruas Moraes[2]

[1]Rio Verde University (FESURV), Faculdade de Medicina Veterinária.
[2]Department of Veterinary Pathology, São Paulo State University, Jaboticabal, São Paulo, Brazil.
* **Corresponding Author:** UNESP/Jaboticabal, Department of Veterinary Pathology, 14884-900, Jaboticabal/SP, Brazil.
E-mail: julietaengracia@gmail.com

Abstract

In this research we studied the alterations in the muscles and myotendinous junction of dogs with muscular dystrophy. Gastrocnemius muscle (GM) and myotendinous junction (MTJ) samples of 3 controls and 6 dystrophic dogs were subjected to histopathological and immunohistochemical assays. Histopathological/histomorphometric analysis showed that the lesions in the GM were more pronounced and showed the highest percentage of Fiber Type II (FTII) and low values for the minimum diameters and areas of Fiber Type I (FTI) and FTII than those in the MTJ. FTII in dystrophic MTJ was morphologically similar to the controls. There was a significant difference (p < 0.07) in the MHCI antigen compared to the control. We conclude that the preservation of the morphological features of the MTJ can be directly related to a better stabilization of FTII, lower expression of the MHCI complex and less cytotoxic activity of CD8.

Key words: dogs, miopathy, Duchenne muscular dystrophy, immunohistochemistry, canine muscular dystrophy.

Introduction

Duchenne Muscular Dystrophy (DMD) is an inherited myopathy characterized by progressive weakness and muscle degeneration in humans (3, 23). The cause of DMD is a deletion in an X chromosome gene, which is responsible for the synthesis of dystrophin (23, 45). Dystrophin-deficient muscle fibers lack the normal interaction between the sarcolemma and the extracellular matrix and due to the weak anchoring muscles suffer ruptures under the repeated stress of contractions (48).

Golden Retriever dogs with muscular dystrophy (GRMD) are the most appropriate experimental models to study the disease because the muscular alterations in GRMD are similar to those described for DMD in humans (13, 14, 24, 41). Lesions, such as degeneration, necrosis, and fibrosis in skeletal muscle are observed in GRMD and

DMD patients (48). Moreover, in both GRMD and DMD patients, death is caused by cardiorespiratory failure (41, 53).

The absence of dystrophin may also affect other structures, including the myotendinous junction (MTJ) and tendon (32). The MTJ is the interface between the skeletal muscle and the tendon, and it is formed by deep longitudinal fissures that are shaped like human fingers and filled with collagen from the tendon (32). The anatomical connection between the muscle cells and the extracellular region in the MTJ is adapted to reduce mechanical stress (26, 27, 33). Type II muscle fibers in this region have interdigitations that are smaller and thinner than those of type I muscle fibers, increasing the contact area with the tendon by 30% to 40%. (29, 33).

In general, two types of muscle fibers are found in the skeletal muscles of adult dogs: type I (FTI) and type II

Beretta et al.; **Immunohistochemical and Morphometric Evaluation of Gastrocnemius Muscle and Myotendinous Junction of Golden Retriever Dogs with Muscular Dystrophy**. Braz J Vet Pathol, 2014, 7(2), 70 - 81

71

(FTII) (26). The morphological constitution of muscle fibers is characterized by the enzyme activity of myosin adenosine triphosphatase (mATPase) (12). Under optical microscopy, FTI stain palely whereas FTII stain darkly (15). In the gastrocnemius muscle (GM), the number of FTI and FTII are similar and was not influenced by the weight of the animals (5, 6).

Studies of dystrophic muscle have indicated that several factors are related to cell death, including mechanical injury, the action of free radicals, the presence of myeloid cells and autoimmunity mediated by T cells (8, 20, 22, 35). The use of immunosuppressants, such as prednisone and tumor necrosis factor-α (TNFα) blockers, in DMD patients and mdx mice has demonstrated that autoimmunity plays an important role in dystrophic muscle lesions. However, the central role of immune cells in DMD, including their activity and activation, has not been fully elucidated (47, 49).

Within this context, the aim of this study was to describe the distribution patterns of FTI, FTII, and lesions present in the GM and MTJ in GRMD by means of immunohistochemical, histochemical, and morphometric analyses.

Material and Methods

Animals

This work fully complies with the ethical principles for animal experimentation adopted by the Brazilian Society of Laboratory Animal Science (SBCAL) and was approved by the Ethics Committee on Animal Use (CEUA) of the São Paulo State University, Jaboticabal, São Paulo, Brazil, protocol number 025486/09.

Six, male Golden Retrievers affected by progressive muscular dystrophy and three, healthy, control, male, mongrel dogs that were negative for the disease were used in this study. The ages of the dogs ranged from 10 to 21 months old. The animals were from the Brazilian Association of Friends of Muscular Dystrophy (AADM) colony based in Ribeirão Preto, São Paulo, Brazil. Muscular dystrophy was confirmed by DNA analysis of leukocyte broth, which was conducted at the Human Genome Study Center in São Paulo and at the AADM Gene Therapy Center.

The dystrophic animals used in the present work died naturally from progressive worsening of the disease. The control animals died of various causes that did not involve the musculoskeletal system.

Analysis of genomic DNA

The genomic DNA was analyzed at the Human Genome Study Center at the University of São Paulo. To perform the analyses, DNA was extracted from blood samples collected from young pups, using a commercial kit (GFX Genomic Blood DNA Purification Kit,

Amersham Pharmacia Biotech, Milwaukee, WI). The genotypes of the dystrophic and nondystrophic dogs were determined using the GF2 and GR1 primers.

Collection and processing of muscle samples

Muscle samples of nondystrophic and dystrophic dogs were collected just after death. Seventy-five fragments of the GM and MTJ were collected in duplicate. Half of the samples were fixed in 10% buffered formalin at pH 7.4 for a period of 24 h, then processed using standard techniques for paraffin embedding, and cut into 5-µm thick sections. The remaining fragments were immersed in n-hexane (Labsynth Co., Diadema, São Paulo, Brazil) and then frozen and stored in liquid nitrogen at -120°C. Subsequently, serial transversal sections were cut (thickness of 5 µm) in a cryostat at -20°C (Damon/IEC Division 3398 Microtome Cryostat), placed on electrically charged adhesive slides (Star Frost adhesive slides, Code 9546, Sakura Finetek Europe, Zoeterwoude, The Netherlands), and stored at -80°C.

Qualitative analysis

After standard histological processing, the GM an MTJ sections were mounted on histologic slides and stained using hematoxylin and eosin (HE) and modified Gomori trichrome (MGT). To characterize the histopathologic changes, a qualitative analysis method was used to take into consideration the percentage of altered muscle fibers in relation to the muscle fascicle. The histopathologic changes were graded as follows:
Grade 0: normal muscle without the presence of abnormalities;
Grade 1: mild lesions, randomly affecting less than 10% of the muscle fibers in each muscle fascicle;
Grade 2: moderate lesions with multifocal distribution affecting 10–50% of the fibers in each muscle fascicle;
Grade 3: severe lesions with diffuse distribution of lesions, affecting more than 50% of the fibers in each muscle fascicle.

Evaluation of collagen type

Picrosirius red staining was used to identify the type of collagen in the MTJ of dystrophic and nondystrophic animals. Collagen type I presented a yellow, orange, or red color, while collagen type III stained green. Collagen type II is present only in cartilage.

Paraffin sections were stained with Sirius red (Code 35780, Sigma-Aldrich Chemical Co., St. Louis, MO, USA) dissolved in a solution of saturated picric acid. The slides were examined under light microscopy (halogen lamp) with a polarizing filter.

Evaluation of intracellular calcium

Slides with frozen sections were stained with Alizarin Red S (ARS; pH 4.3), specifically to evaluate

Beretta et al.; **Immunohistochemical and Morphometric Evaluation of Gastrocnemius Muscle and Myotendinous Junction of Golden Retriever Dogs with Muscular Dystrophy**. Braz J Vet Pathol, 2014, 7(2), 70 - 81

72

calcium. The intracellular calcium stained orange-red. The relative proportions of calcium-positive muscle fibers (orange-red stained) and calcium-negative fibers (unstained) in the GM and MTJ of the two groups (dystrophic and nondystrophic) were evaluated. In this histopathological evaluation, 200 muscle fibers of the GM and MTJ were randomly analyzed to assess the percentages of ARS-positive and ARS-negative fibers in each sample.

Histomorphometric analysis

Frozen sections were used to perform the mATPase reaction (adenosine 5'-triphosphate from Sigma-Aldrich Diagnostics, St. Louis, MO, USA) with alkaline pre-incubation (pH 9.4) to evaluate the percentage and distribution of FTI and FTII in GM and MTJ.

Morphometric analyses of the diameters and areas of the FTI and FTII were performed using an image analyzer (KS 100 version 3.0, Kontron, Carl Zeiss). Images were obtained by a video camera (Color Video Camera TK-1070U-JVC) attached to a binocular microscope (Jenaval, Carl Zeiss) and connected to a microcomputer. A total of 100 fibers of each type (FTI and FTII) were randomly analyzed for each sample (GM and MTJ) from the dystrophic and nondystrophic animals. The minimum diameter and area were calculated as the arithmetic mean of the values obtained.

Immunohistochemistry

Six primary antibodies were used to determine the expression of CD4, CD8, major histocompatibility complex MHCI, MHCII, utrophin and vimentin in the dystrophic and nondystrophic animal samples with immunohistochemical assays using streptavidin-biotin peroxidase complexes with modifications (Hsu et al. 1981) (Table 1).

For the paraffin sections, the slides were initially kept in a dry oven for 1 h at 60°C, followed by deparaffinization in xylene and decreasing concentrations of ethyl alcohol. Each of the steps was preceded by rinsing with Tris-HCl buffer (pH 7.6).

For the reactions with the anti-MHCII and anti-vimentin antibodies, antigen retrieval was performed in an electric steamer at 97°C (Cuis Steamer T-Fal, Arno SA) with a pre-warmed solution of 10 mM sodium citrate (pH 6.0). To block endogenous peroxidase activity, hydrogen peroxide was added to a solution of phosphate-buffered saline (PBS; pH 7.4), for a final concentration of 5%. Nonspecific reactions were blocked with 2% bovine serum albumin (BSA; A7030, Sigma). Primary antibodies were diluted in 1% BSA and incubated in a humidified chamber at 4°C for 16 h.

The labeled polymer EnVision (EnVision + Dual Link Kit HRP, Dako, catalog #K4061) was used as the secondary complex. The reactions were developed using 3,3-diaminobenzidine (Liquid DAB+, Dako K3468-1) as the chromogenic substrate, counterstained with Harris hematoxylin for 30 s, and then rinsed in running water.

The sections were dehydrated in increasing gradients of ethyl alcohol, followed by a clearing step in xylene. Permount was used to mount the coverslips (SP15-500, Fisher Scientific).

For immunohistochemical reactions with the anti-CD4, anti-CD8, anti-MHCI and anti-utrophin antibodies, the frozen sections were fixed in cold acetone and then washed with Tris buffered saline with Tween (TBST; pH 7.6). From this stage forward, the immunohistochemistry procedures followed the protocol developed for paraffin sections, starting at the step for blocking endogenous peroxidase activity.

For the anti-CD4 and anti-CD8 antibodies, all immunostained cells were randomly counted in five fields for each section with the assistance of a graticule micrometer (Nikon, Inc., Japan) at 400× magnification. For the other antibodies, the distribution and presence in the tissues was examined and scored as follows: (0) no immunostaining; (1) weak; isolated, and randomly distributed immunostaining; (2) moderate; immunostaining in groups with multifocal distribution, and (3) strong; diffuse immunostaining throughout the muscle section.

Statistical analysis

The Kruskal-Wallis test (p ≤ 0.07) was used to analyze all immunostaining reactions. The least squares method was used to compare the minimum diameters and areas of the FTI and FTII, and the Wilcoxon test was used to compare distributions of fiber types (p ≤ 0.05 for both tests). All statistical analyses were performed using SAS software (SAS 9.1, SAS Institute, Cary, NC, USA).

Results

Qualitative analysis

In the nondystrophic dogs, the GMs and MTJs had uniformly distributed muscle fibers. They had a polyhedral cellular arrangement and scarce interfibrillar space interspersed with connective tissue. Morphological changes were observed in the dystrophic animals, including increased endomysial and perimysial spaces with fibrous replacement, low fat infiltration and a considerable number of mononuclear inflammatory cells. The myofibers were altered in shape and diameter, showing atrophy and/or hypertrophy. Hyalinized fibers exhibited hyperacidophilic, hypertrophied, and clear and well-defined cytoplasm. In the GM, clustered necrotic fibers with cytoplasmic deformities, pale and homogeneous sarcoplasm, pyknotic nuclei and the presence of phagosomes with cellular debris were evident. In both the GM and MTJ, fibers with basophilic cytoplasm and large nuclei were identified, suggesting regeneration processes

Beretta et al.; **Immunohistochemical and Morphometric Evaluation of Gastrocnemius Muscle and Myotendinous Junction of Golden Retriever Dogs with Muscular Dystrophy**. Braz J Vet Pathol, 2014, 7(2), 70 - 81

73

(Figure 1A). The observed ragged red fibers were characterized by a granular red-blue appearance in the sarcoplasm from the MGT staining (Figure 1B).

Moderate lesions (Grade 2) affecting 10–50% of the myofibers in each muscle band were observed in the gastrocnemius muscle of 83% of the dystrophic animals. The remaining animals (17%) showed severe lesions (Grade 3), with diffuse, damaged myofibers that affected more than 50% of the muscle fibers in each band (Table 2).

Discrete lesions were observed in the MTJs of all dystrophic animals. Damaged myofibers were isolated and randomly distributed (Grade 1) in 50% of the animals and moderate lesions were observed in the remaining 50% (Grade 2) (Table 2).

Evaluation of collagen type

The types of collagen present in the MTJ of the dystrophic and nondystrophic animals did not differ.

Interdigitations formed by deep longitudinal fissures of muscle tissue were observed, intermingled with type I collagen and with fibers arranged in reddish colored bundles coming from the tendon (Figure 2).

Evaluation of intracellular calcium

Dystrophic calcification of muscle fibers in the necrotic regions was observed with ARS staining. Calcium was distributed evenly throughout the myofiber sarcoplasm. Isolated fibers and/or areas with a concentration of ARS-positive fibers were seen in the GMs and MTJs of all dystrophic animals (Figure 3A). The Kruskal-Wallis test indicated no significant correlation ($p < 0.05$) between the number of ARS-positive fibers in the GM or MTJ of dystrophic and non-dystrophic dogs (Figure 3B).

Table 1. Specifications of the primary antibodies used in the immunohistochemical assay of dystrophic and non-dystrophic animals muscle samples.

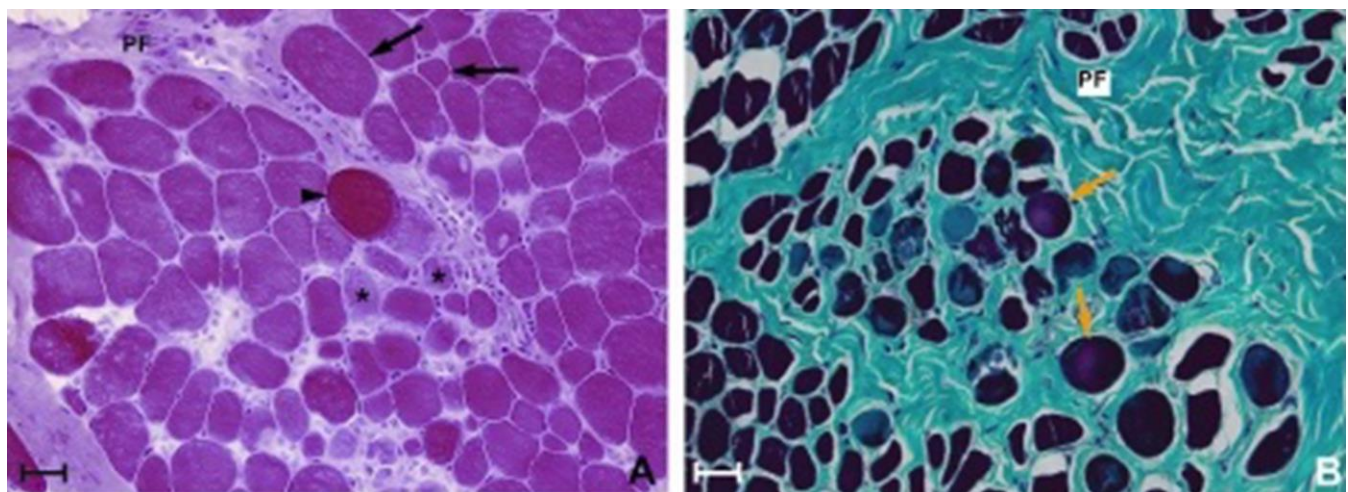| Primary antibodies	Sample	Dilution	Code	Brand	Control
Anti-CD4	Paraffin	1/80	DH29A	VRMD	Lynph node
Anti-CD8	Paraffin	1/80	CADO46A	VRMD	Lynph node
Anti-MHCI	Paraffin	1/240	H 58	VRMD	Colon
Anti-MHCII	Frozen	1/400	M0746	Dako	Lynph node
Anti-utrophin	Paraffin	1/200	NCL-DRP2	Novo Castra	Neuromuscular junction
Anti-vimentin	Frozen	1/200	M7020	Dako	Utero

Figure 1. Gastrocnemius muscle and myotendinous junction of dystrophic dogs. **A**. Myofibers with variations in diameter (arrows), necrotic fiber (*), perimysial fibrosis (PF) and hyalinized fiber (H). HE. Bar = 10 μm. **B.** "Ragged red" fiber (arrows) and perimysial fibrosis (PF). MGT. Bar = 10 μm. **C.** Calcification of the myofiber (arrows). ARS. Bar = 10 μm.

Beretta et al.; **Immunohistochemical and Morphometric Evaluation of Gastrocnemius Muscle and Myotendinous Junction of Golden Retriever Dogs with Muscular Dystrophy**. Braz J Vet Pathol, 2014, 7(2), 70 - 81

74

Table 2. Percentage of degrees of injuries on the gastrocnemius muscle and myotendinous junction in dystrophic dogs.

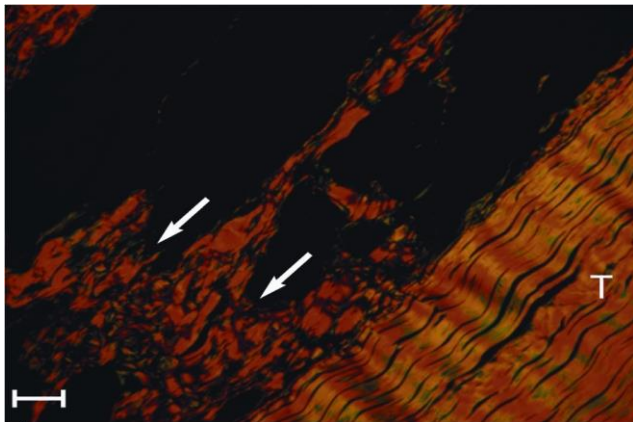| Degree	Gastrocnemius muscle	Myotendinous junction
1	0.0%	50.0%
2	83%	50.0%
3	17%	0.0%

Figure 2. Myotendinous junction of dystrophic dog. Parallel collagen fibers of tendon (T) and interdigitation of muscle tissue and collagen (arrows). Picrosirius red staining under polarized light microscopy. Bar = 5 μm.

Histomorphometric analysis

The GM and MTJ muscle fibers in the nondystrophic animals showed a mosaic pattern with a homogeneous distribution of FTI and FTII. However, the dystrophic fibers had irregular edges and a diversity of size, and they displayed grouping by type of FTIs and FTIIs. In dystrophic GMs, FTIIs were predominant, whereas FTIs were predominant in the nondystrophic animals (Figures 4 A, B, C).

The proportion of FTI to FTII in the MTJs of the dystrophic and nondystrophic groups did not differ (Figure 4C). The mean FTI and FTII minimum diameters and areas were significantly smaller in dystrophic fibers than in the nondystrophic fibers (p < 0.05). The mean FTI minimum diameter and area in the dystrophic group were less than those observed in the nondystrophic group (p < 0.05), whereas there were no significant differences found between groups in the mean FTII minimum diameter and area (Figure 4D, E).

Immunohistochemistry

Immunostaining of CD4$^+$ and CD8$^+$ lymphocytes

CD4$^+$ and CD8$^+$ lymphocytes were isolated and randomly distributed throughout the endomysium, perimysium, and around vessels in the nondystrophic animals. In dystrophic animals, these lymphocytes were also observed in areas of degeneration and necrosis (Figure 5A and 5B). A significantly greater number of CD4$^+$ and CD8$^+$ cells was observed in dystrophic muscles when compared to nondystrophic muscles (p < 0.07). However, the numbers of CD4$^+$ and CD8$^+$ lymphocytes between the GMs and MTJs of dystrophic animals did not differ (Table 3).

Immunostaining of MHCI and MHCII antigens

Immunostaining of the MHCI antigen occurred in the capillaries and blood vessels of the endomysium and perimysium in the nondystrophic GMs and MTJs. In the dystrophic muscles, MHCI was also expressed in areas of inflammation, necrosis, and regeneration, as well as on the surface of myofibers. MHCI staining was significantly different between the GM and the MTJ, with strong immunostaining (score 3) in the GM (Figure 5C) and moderate immunostaining (score 2) in the MTJ (Figure 5D) (p < 0.07) (Table 4).

The pattern of MHCII immunostaining was similar to that of MHCI, with positive staining in blood vessels and mononuclear endomysial cells of the nondystrophic animals. In the dystrophic muscles, mononuclear endomysial cell macrophages were also present in regions of inflammation undergoing necrosis and degeneration (Figure 5E and 5F).
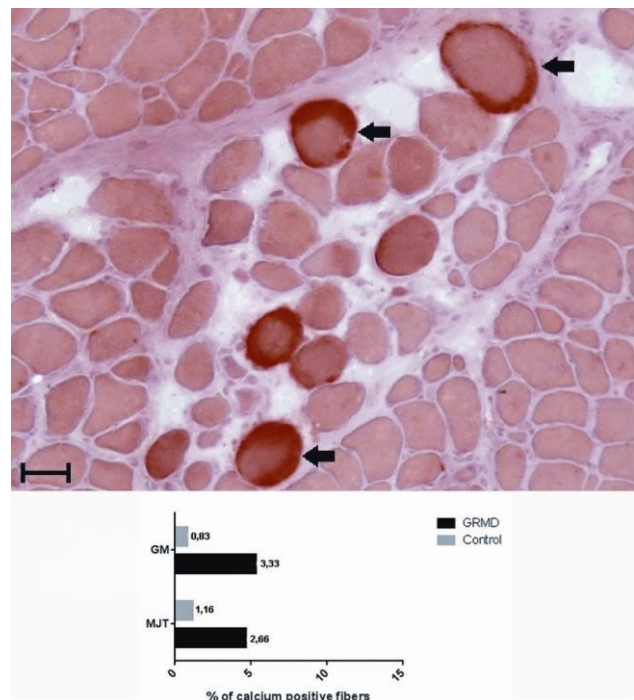

Figure 3. A. Gastrocnemious muscle of a dystrophic dog with calcium-positive fibers showing intracellular orangish-red staining (arrows). ARS. Bar = 10 μm. **B.** Percentage of ARS positive fibers in the gastrocnemius muscle (GM) and myotendinous junction (MJT) of dystrophic and non-dystrophic dogs.

Beretta et al.; **Immunohistochemical and Morphometric Evaluation of Gastrocnemius Muscle and Myotendinous Junction of Golden Retriever Dogs with Muscular Dystrophy**. Braz J Vet Pathol, 2014, 7(2), 70 - 81

75

The average immunostaining ranged from weak to moderate (scores 1 and 2, respectively) and was more severe in the GM. However, no statistically significant difference between the dystrophic GMs and MTJs was observed (p < 0.07) (Table 5).

Vimentin immunostaining

In the nondystrophic animals, vimentin expression was strong in the blood vessels and weak in the connective tissue. The degree of immunostaining was strong (score 3) in dystrophic GMs and moderate (score 2) in dystrophic MTJs. Vimentin was largely expressed in regenerating myofibers and was observed in areas of degeneration, necrosis, and inflammation (Figures 5G and 5H). There was no statistical difference between vimentin staining in the MTJs and the GMs of dystrophic cells (Table 4).

Immunostaining of utrophin

In the nondystrophic animals, utrophin immunostaining was intense in blood vessels and was expressed with weak intensity (score 1) on the surface of GM and MTJ muscle cells (Figure 5I). In dystrophic cells, the degree of immunostaining was strong (score 3) on the surfaces of the myofibers and blood vessels as well as in the sarcoplasm of some regenerating myofibers in the GMs and MTJs (Figure 5J).

Discussion

In this study, the histopathological analysis demonstrated that the GMs and the MTJs of dystrophic animals have alterations characteristic of muscular dystrophy in human beings, such as fibrosis, hyalinization, hypertrophy, ragged red fibers, necrosis, calcification, and regeneration. These results corroborate those reported for dystrophic dogs by other authors (31, 38, 41). We found no significant differences in the percentages of ARS-positive fibers between the dystrophic and nondystrophic dogs in the MTJ and GM. These findings differed from those of earlier studies showing a significant difference in the level of calcium-positive fibers between the dystrophic and nondystrophic groups for five muscles. In particular, in a previous study of 1- to 51-month-old GRMD, the masseter, brachial biceps and triceps, femoral biceps, and cranial sartorius presented a greater number of ARS-positive fibers in comparison to nondystrophic dogs (39). The results suggest that the MTJ and GM are more preserved than other muscles in GRMD. Moreover, the morphological lesions in the MTJ were more attenuated than in the GM.

There was no difference in the type of collagen present in the MTJs of dystrophic and normal animals. Evidence of collagen fibers with high birefringence and a strong reddish staining was found in both groups, which is typical of type I collagen normally found in the MTJ (28, 40, 43), indicating that no significant changes occurred in this region.

The formation of groupings by type of FTI and FTII was observed in the GMs and MTJs of dystrophic dogs, as previously described in GRMD by other authors (31, 38, 52). This type of lesion is reported only in dogs and can be used as a characteristic marker of the disease (52). The fiber type composition in the dystrophic dogs was also altered.

Table 3. Mean and standard error of the number of CD4$^+$ and CD8$^+$ by 0.0052 mm^2 in the gastrocnemius muscle and myotendinous junction of non-dystrophic and dystrophic dogs.

Groups	Gastrocnemius muscle		Myotendinous junction	
	CD4$^+$	CD8$^+$	CD4$^+$	CD8$^+$
Dystrophic	31.66 ± 4.88 (a)	35.50 ± 6.22 (a)	27.33 ± 3.26 (a)	31.33 ± 6.21 (a)
Non-dystrophic	1.66 ± 0.57 (b)	2.00 ± 0.02 (b)	1.33 ± 0.57 (b)	2.00 ± 1.00 (b)

Means followed by different letters indicate significant differences (P < 0.07) by the method of Kruskal-Wallis.

Table 4. Mean and standard error, minimum and maximum score for immunostaining of the MHCI antigen in gastrocnemius muscle and myotendinous junction of dystrophic dogs.

	MHCI	MHCII	Vimentin
Sample	**Mean ± SD**		
Gastrocnemius muscle	2.75 ± 0.27 (a)	1.83 ± 0.60 (a)	2.83 ± 0.40 (a)
Myotendinous junction	2.33 ± 0.40 (b)	1.33 ± 0.75 (a)	2.33 ± 0.75 (a)

Means followed by different letters in the column indicate significant differences (P <0.07) by the method of Kruskal-Wallis. SD: standard error.
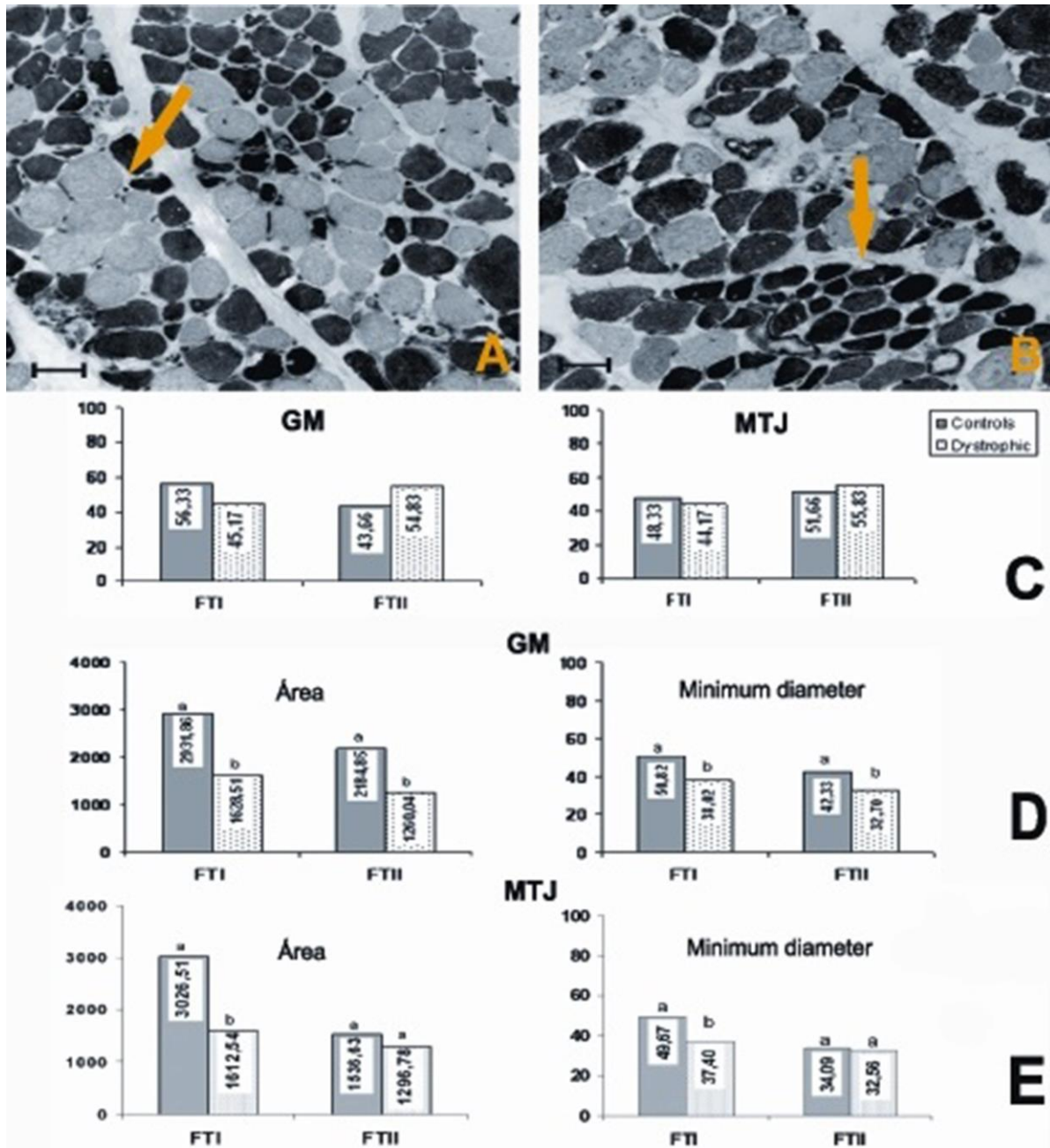
Beretta et al.; **Immunohistochemical and Morphometric Evaluation of Gastrocnemius Muscle and Myotendinous Junction of Golden Retriever Dogs with Muscular Dystrophy**. Braz J Vet Pathol, 2014, 7(2), 70 - 81

76

Figure 4. Enzymo histochemistry mATPase reaction (pH 9.4). **A.** Myotendinous junction of dystrophic dog with type-grouping of FTI (arrow). **B.** Gastrocnemius muscle of dystrophic dogs: type-grouping of FTII (arrow). **C.** Graphical representation of percentage of FTI and FTII in the gastrocnemius muscle and myotendinous junction of non-dystropic and dystrophic dogs. **D.** Graphical representation of mean area and the minimum diameter in micrometers of FTI and FTII in gastrocnemius muscle of control and of dystrophic dogs. **E.** Graphical representation of mean area and the minimum diameter in micrometers of FTI and FTII in the myotendinous junction of non-dystrophic and of dystrophic dogs. Means followed by different letters indicate significant differences (P < 0.05) by the method of least squares. Bar = 10 µm.
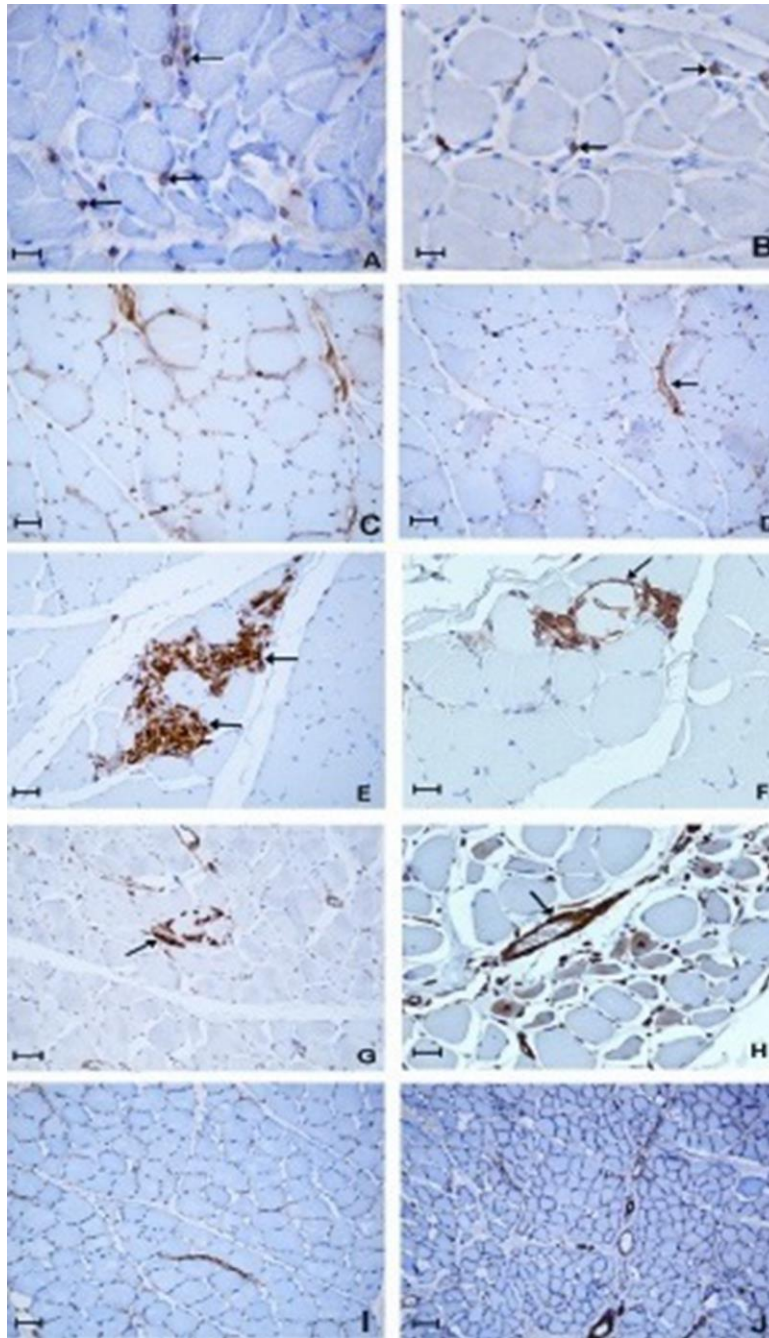
Beretta et al.; **Immunohistochemical and Morphometric Evaluation of Gastrocnemius Muscle and Myotendinous Junction of Golden Retriever Dogs with Muscular Dystrophy**. Braz J Vet Pathol, 2014, 7(2), 70 - 81

77

Figure 5. **A/B.** Immunohistochemical reaction for T lymphocytes in the gastrocnemius muscle of dystrophic dogs. CD8^{+} immunostaining (arrows) (A). CD4^{+} immunostaining (arrows) (B). Bar = 5 μm. **C/D.** Immunohistochemical reaction for MHCI in the gastrocnemius muscle and myotendinous junction of dystrophic dogs; immunostaining at the sarcolemma (*) and blood vessels (arrow). Gastrocnemius muscle: moderate immunostaining. Myotendinous junction, weak immunostaining (D). Bar = 10 μm. **E/F.** Immunohistochemical reaction for MHCII in the gastrocnemius muscle and myotendinous junction of dystrophic dogs. E: Gastrocnemius muscle: immunoreactivity in mononuclear cells (arrows). Bar = 10 μm. F: Myotendinous junction: immunostaining in the sarcolemma (arrow) in area of necrosis. Bar = 5 μm. **G.** Immunohistochemical reaction for vimentin in the myotendinous junction of dystrophic dogs. Immunostaining in necrotic area (arrow). Bar = 5 μm. **H.** Immunohistochemical reaction for vimentin in the gastrocnemius muscle of dystrophic dogs. Immunostaining in regenerating myofibers (*) and blood vessels (arrow). Bar = 5 μm. **I/J.** Immunohistochemical reaction for utrophin.. I: Myotendinous junction of non-dytrophic dogs: blood vessel (strong immunostaining near center), weak immunostaining for utrophin at the sarcolemma. Bar = 10 μm. J: Myotendinous junction of dystrophic dogs: blood vessel (strong immunostaining under center), strong immunostaining for utrophin at the sarcolemma. Bar = 20 μm.

Beretta et al.; **Immunohistochemical and Morphometric Evaluation of Gastrocnemius Muscle and Myotendinous Junction of Golden Retriever Dogs with Muscular Dystrophy**. Braz J Vet Pathol, 2014, 7(2), 70 - 81

78

Table 5. Mean and standard error, minimum and maximum score for immunostaining of the MHCII antigen in gastrocnemius muscle and myotendinous junction of dystrophic dogs.

Sample	Mean ± SD
Gastrocnemius muscle	1.83 ± 0.60 (a)
Myotendinous junction	1.33 ± 0.75 (a)

Means followed by different letters indicate significant differences (P <0.07) by the method of Kruskal-Wallis. SD: standard error.

Table 6. Mean and standard error, minimum and maximum score for immunostaining of vimentin antigen in gastrocnemius muscle and myotendinous junction of dystrophic dogs.

Sample	Mean ± SD
Gastrocnemius muscle	2.83 ± 0.40 (a)
Myotendinous junction	2.33 ± 0.75 (a)

Means followed by different letters indicate significant differences (P <0.07) by the method of Kruskal-Wallis. SD: standard error.

In the GMs of the dystrophic dogs, the slow contracting FTI was replaced by fast contracting FTII, and in the MTJ, the number of FTII increased. In our previous study of 7- to 13-month-old GRMD, FTII was replaced by FTI in six muscles (i.e., the masseter, semimembranosus, biceps femoris, cranial sartorius, biceps, and triceps brachii).

The fiber types of the skeletal musculature are controlled by nerve activity through specific signaling pathways, such as the calcineurin (Cn)-nuclear factor of activated T-cells (NFAT) pathway. The Cn-NFAT pathway the principal signaling route responsible for maintaining the activity of genes that produce slow contraction fibers in adult muscles and during regeneration of these muscles (31). Studies showed that there is an attenuated form of the disease in lines of dystrophic mdx mice with enhanced activity of the Cn pathway because FTI may express greater quantities of utrophin, a membrane protein that compensates for the lack of dystrophin (4, 19, 49). However, even though the 7- to 13-month-old GRMD had a higher proportion of FTI, they had more severe histopathologic alterations. In the present study, dystrophic animals showed an increased number of FTII and more moderate histopathologic lesions. Thus, taken together, these data still do not support a role for FTI predominance in GRMD.

The average minimum diameter and area of FTII in the MTJs were equal to those observed in the normal animals, suggesting that visible atrophic or hypertrophic lesions were absent. This result suggests that the larger contact area of FTII (29, 32) and the connection between muscle fibers and tendons mediated by integrin (37) generates greater stability in the MTJ, preserving it from the stress of contraction.

Utrophin was strongly expressed in both structures studied, corroborating what has been previously described for the soleus and the extensor digitorum longus muscles (9, 10), as well as the MTJs of dystrophic mice (37, 42, 54). The MTJ appeared more morphologically preserved than the GM. These data coupled with the predominance of fiber type and morphological lesions suggest that utrophin is not the only stabilizing protein acting in this region. Therefore, joint action with another protein normally found in the MTJ, such as integrin, may play an important role in the organizational and structural maintenance of this region and could explain the milder lesions found in these areas.

The significant increase in CD4$^+$ and CD8$^+$ cells in the dystrophic fibers strongly suggests the action of the immune system in the inflammatory process in GRMD, corroborating other studies on human patients with DMD (7, 35) and on GRMD (38). There was no statistical difference between the number of CD4$^+$ and CD8$^+$ cells in the GMs and MTJs of dystrophic animals. These findings contradict studies describing a predominance of CD4$^+$ and CD8$^+$ cells in the muscles of mdx mice (2, 16, 17, 46), GRMD (38), and humans with DMD (35). However, the results reinforce previous findings demonstrating that lymphoid infiltrates have variable locations and intensities in dystrophic canine muscle tissue (14).

The similar number of CD4$^+$ and CD8$^+$ cells indicates that there is a joint action of these cells in dystrophic muscle, without one cell type overpowering the other. An interaction between CD4$^+$ and CD8$^+$ cells has been reported in studies of mdx mice, where the cytokine interleukin-2 released by CD4$^+$ cells acted favorably on CD8$^+$ cell proliferation (50, 21).

MHCII immunoreactivity in dystrophic cells ranged from weak to moderate; it was observed in macrophages and areas of necrosis and degeneration, corroborating studies that have reported its expression in GRMD (38) and humans with DMD (14, 30). MHCII is responsible for the appearance and activation of CD4$^+$ cells, which activate potent microbicidal substances that destroy phagocytosed pathogens when associated with macrophages (47). Thus, in this study, there was evidence that CD4$^+$ lymphocytes can activate macrophages and induce CD8$^+$ cell migration, similar to the results observed for other muscles in GRMD (38).

The expression of MHCI was detected on the surface of dystrophic myofibers and in areas of necrosis, regeneration, and inflammation. These findings agree with those reported for the vastus lateralis, rectus femoris, deltoid, and quadriceps muscles in human patients with DMD (1, 16, 30, 35), as well as with the results reported for the masseter, diaphragm, biceps brachii, long head of triceps brachii, semitendinosus, semimembranosus, superficial head of the biceps femoris, and cranial sartorius muscles in GRMD (38). The degree of MHCI expression was more moderate in dystrophic MTJ cells than in GM cells. Its presence in the target cells is essential for the

Beretta et al.; **Immunohistochemical and Morphometric Evaluation of Gastrocnemius Muscle and Myotendinous Junction of Golden Retriever Dogs with Muscular Dystrophy**. Braz J Vet Pathol, 2014, 7(2), 70 - 81

79

cytotoxic activity of CD8^{+} lymphocytes (34, 36). Under these conditions, the lower expression of MHCI in MTJ myofibers may be related to decreased activation of CD8^{+} cells and consequently less damage to myofibers. However, other factors, such as cytokines and costimulatory molecules, may contribute to this reduction.

The immunoexpression of vimentin was intense in the MTJs and GMs of dystrophic muscles. The presence of this protein has also been reported in the dystrophic muscles of humans with DMD (18). Vimentin acts in the regenerative process and is responsible for the migration, fusion, and structural modeling of myogenic cells (11, 51). The strong intensity of immunostaining observed in this study disagrees with other studies of GRMD, in which vimentin was expressed weakly in the eight muscles examined (38). These findings suggest that the GM and the MTJ maintain their regenerative capacity even in the final stages of the disease.

Considering the morphofunctional preservation of the MTJ observed in this study, a number of factors may act together. One factor is greater anchoring of FTII in the MTJ, causing less severe lesions and a lower release of cytosolic proteins. Therefore, there is lower MHCI-peptide complex expression, which is responsible for the presence and activation of cytotoxic T cells in the muscle to modulate the myofiber lesions.

We conclude that morphological preservation of the MTJ may be directly related to better stabilization of FTII, lower expression of the MHCI, and decreased immune system activity. Studies on the morphological conservation of FTII and the immune system in the MTJ are still needed, but these results support investigations of GRMD physiopathogenesis.

Acknowledgments

References

1. APPLEYARD ST., DUNN JJ., DUBOWITZ V., ROSE ML. Increased expression of the HLA abc class I antigens by muscle fibers in Duchenne muscular dystrophy inflammatory myopathy and other neuromuscular disorders. **Lancet**, 1985, 16, 361-3.
2. ARAHATA K., ENGEL AG. Monoclonal antibody analysis of mononuclear cells in myopathies I Cell-mediated cytotoxicity and muscle fiber necrosis. **Ann. Neurol.**, 1988, 23, 168-73.
3. BAROHN RJ. Muscular dystrophys. BENNETT JC, GOLDMAN LC. Eds. **Tratado de medicina interna**. 21.ed. Rio de Janeiro: Guanabara Koogan, 2001, 2458-62.
4. BERGMAN RL., INZANA KD., MONROE WE., SHELL LG., LIU LA., ENGVALL E., SHELTON GD. Dystrophin-deficient muscular dystrophy in a Labrador retriever. **J. Am. Anim. Hosp. Assoc.**, 2002, 38, 255-61.
5. BRAUNT KG., HOFF EJ., RICHARDSON KEY. Histochemical identification of fiber types in canine skeletal muscle **Am. J. Vet. Res.**, 1978, 39, 561-65.
6. BRAUNT KG., LINCOLN CE. Histochemical differentiaton of fiber types in neonatal canine skeletal muscle. **Am. J. Vet. Res.**, 1981, 42, 407-15.
7. BRUNELLI S., ROVERE-QUERINI P. The immune system and the repair of skeletal muscle. **Pharmacol. Res.**, 2008, 58, 117-21.
8. CAI B., SPENCER MJ., TSENG-ONG L., NAKAMURA G., TIDBALL JG. Eosinophilia of dytrophin-deficient muscle is promoted by perforin-mediated cytotoxicity by T cells effectors. **Am. J. Pathol.**, 2000, 156, 1789-96.
9. CHAKKALAKAL J., HARRISON MA., CARBONE TTO S., CHIN E., MICHEL RN., JASMIN BJ. Stimulation of calcineurin signaling attenuates the dystrophic pathology in mdx mice. **Hum. Mol. Genet.**, 2004, 13, 379-88.
10. CHAKKALAKAL J., MICHEL SA., CHIN ER., MICHEL RN., JASMIN BJ. Targeted inhibition of Ca^{2+}/calmodulin signaling exacerbates the dystrophic phenotype in mdx mouse muscle. **Hum. Mol. Genet.**, 2006, 15, 1423-35.
11. CHARGÉ SBP., RUDNICKI MA. Cellular and Molecular Regulation of Muscle Regeneration. **Physiol. Rev.**, 2004, 1, 209-38.
12. CLOSE RI. Dynamic properties of mammalian skeletal muscles. **Physiol. Rev.**, 1972, 52, 129-97.
13. COLLINS CA., MORGAN JE. Duchenne's muscular dystrophy: animal models used to investigate pathogenesis and develop therapeutic strategies. **Int. J. Exp. Pathol.**, 2003, 84, 165-72.
14. COOPER BJ., WINAND NJ., STEDMAN H., VA LENTINE BA., HOFFMAN EP., KUNKEL LM., SCOTT MO., FISCHBECK KH., KORNEGAY JN., AVERY RJ., WILLIAMS JR., SCHMICKEL RD., SYLVESTER JE. The homologue of the Duchenne locus is defective in X-linked muscular dystrophy of dogs. **Nature**, 1988, 334, 154-6.
15. DUCHENNE GB. Recherches sur la paralysie musculaire pseudo-hypertrophique ou paralysie myosclerosique. **Arch. Gén. Méd.**, 1868, 11, 421-552.
16. EMSLIE-SMITH AM., ARAHATA K., ENGEL AG. Major histocompatibility complex class I antigen expression immunolocalization of interferon subtypes and T cell-mediated cytotoxicity in myopathies. **Hum. Pathol.**, 1989, 20, 224-31.
17. ENGEL AG., ARAHATA K. Mononuclear cells in myopathies: Quantitation of functionally distinct subsets recognition of antigen-specific cell-mediated cytotoxicity in some diseases and implications for the pathogenesis of the different inflammatory myopathies. **Hum. Pathol.**, 1986, 17, 704-21.

Beretta et al.; **Immunohistochemical and Morphometric Evaluation of Gastrocnemius Muscle and Myotendinous Junction of Golden Retriever Dogs with Muscular Dystrophy**. Braz J Vet Pathol, 2014, 7(2), 70 - 81

80

18. GALLANTI A., PRELLE A., MOGGIO M., CISCATO P., CHECCARELLI N., SCIACCO M., COMINI A., SCARLATO G. Desmin and Vimentin as markers of regeneration in muscle diseases. **Acta Neurophatol.**, 1992, 85, 88-92.

19. GASCHEN F., BURGUNDER JM. Changes of skeletal muscle in Young dystrophin-deficient cats: a morphological and morfometric study. **Acta Neuropathol.**, 2001, 101, 591-600.

20. GE Y., MOLLOY MP., CHAMBERLAIN JS., ANDREWS PC. Differential expression of the skeletal muscle proteome in mdx mice at different ages. **Electrophoresis**, 2004, 25, 2576-85.

21. GONZÁLEZ-QUINTIAL R., BACCALÀ R., POPE RM., THEOFILOPOULOS AN. Identification of clonally expanded T cells in rheumatoid arthritis using a sequence enrichment nuclease assay. **J. Clin. Invest.**, 1996, 97, 1335-43.

22. GOROSPE JR., THARP MD., HINCKLEY J., KORNEGAY JN., HOFFMAN EP. A role for mast cells in the progression of Duchenne muscular dystrophy Correlations in dystrophin-deficient human dogs and mice. **J. Neurol. Sci.**, 1994, 122, 44-56.

23. HAYS AR., ARMBRUSTMACHER W. RUBIN E., FARBER JL. **Patologia**. 3.ed. Rio de Janeiro: Guanabara Koogan, 2002, 1363-89.

24. HOWELL JM., FLETCHER S., KAKULAS BA., O'HARA M., LOCHMULLER H., KARPATI G. Use of the dog model for Duchenne muscular dystrophy in gene therapy trials. **Neuromuscul. Disord.**, 1997, 7, 325-8.

25. HSU SM., RAINER L., FANGER HA. A comparative study of the peroxidase-antiperoxidase method and an avidin biotin complex method for studying polypeptide hormones with radioimmunoassay antibodies. **Am. J. Clin. Pathol.**, 1981, 75, 734-38.

26. JÄRVINEN M., KANNUS P., KVIST M., ISOLA J., LEHTO M., JOZSA L. Macromolecular composition of the myotendínous junction. **Exp. Mol. Pathol.**, 1991, 55, 230-7.

27. JÄRVINEN TAH., JOZSA L., KANNUS P, JÄRVINEN TLN, KVIST THM, KALIMO H, JÄRVINEN M. Mechanical loading regulates the expression of tenascin-C in the myotendinous junction and tendon but does not induce de novo synthesis in the skeletal muscle. **J. Cell. Sci.**, 2002, 116, 857-6.

28. JUNQUEIRA LCU., COSSERMELLI W., BRENTANI R. Differential staining of collagens type I, II and III by sirius red and polarization microscopy. **Arch. Histol. Japon.**, 1978, 41, 267-74.

29. KANNUS P., JOZSA L., KVIST M., LEHTO M., JÄRVINEN M. The effect of immobilization on myotendinous junction: a ultrastructural histochemical and immunohistochemical study. **Acta Physiol. Scand.**, 1992, 144, 387-94.

30. KARPATI G., POULIOT Y., CARPENTER S. Expression of immunoreactive major histocompatibility complex products in human skeletal muscles. **Ann. Neurol.**, 1988, 23, 64-72.

31. KORNEGAY JN., TULER SM., MILLER DM., LEVESQUE DC. Muscular dystrophy in a litter of golden retriever dogs. **Muscle Nerve**, 1988, 11, 1056-64.

32. KVIST M., JOZSA L., KANNUS P., ISOLA J., VIENO T., JÄRVINEN M., LEHTO M. Morphology and histochemistry of the myotendineal junction of the rat calf muscles. **Acta Anat.**, 1991, 141, 199-205.

33. LAW DJ., TIDBALL JG. Dystrophin deficiency is associated with myotendinous junction defects in prenecrotic and fully regenerated skeletal muscle. **Am. J. Pathol.**, 1993, 142, 1513-23.

34. MARTZ E., HEAGY W., GROMSOWSKI SH. The mechanism of CTL mediated killing: monoclonal antibody analysis of the roles of killer and target-cell membrane proteins. **Immunol. Rev.**, 1983, 72, 73-96.

35. MCDOUALL RM., DUNN MJ., DUBOWITZ V. Nature of the mononuclear infiltrate and the mechanism of muscle damage in juvenile dermatomyositis and Duchenne Muscular Dystrophy. **J. Neurol. Sci.,** 1990, 99, 199-217.

36. MCMICHAEL AJ. HLA restriction of human cytotoxic T-cells. **Springer Semin. Immunopathol.**, 1980, 3, 3-22.

37. MIOSGE NC., KLENCZAR R., HERKEN M., WILLEM UM. Organization of the myotendinous junction is dependent on the presence of α7 β1 integrin. **Lab. Invest.**, 1999, 79, 1591-9.

38. MIYAZATO LG., MORAES JR., BERETTA DC., KORNEGAY JN: Muscular dystrophy in dogs: does the crossing of breeds influence disease phenotype? **Vet. Pathol.**, 2011, 48, 655-62.

39. MIYAZATO LG., BERETTA DC., ENGRACIA FILHO JR., MORAES FR., MORAES JRE. Evaluation of intracellular calcium in canine muscular dystrophy. **Braz. J. Vet. Pathol.**, 2011, 4, 95-102.

40. MONTES GS. Structural Biology of the fibers of the collagenous and elastic systems. **Cell. Biol. Int.**, 1996, 20, 15-27.

41. NGUYEN F., CHEREL Y., GUIGAND L., GOUBAULT-LEROUX I., WYERS M. Muscles lesions associated with dystrophin deficiency in neonatal Golden Retriever puppies. **J. Comp. Pathol.**, 2002, 126, 100-8.

42. PEARCE M., BLAKE DJ., TINSLEY JM., BYTH BC., CAMPBELL L., MONACO AP., DAVIES KE. The utrophin and dystrophin genes share similarities in genomic structure. **Hum. Mol. Genet.**, 1996, 2, 1765-72.

43. RICH L., WHITTAKER P. Collagen and Picrosirius red staining: a polarized light assessment of fibrilar hue and spatial distribution. **Braz. J. Morphol. Sci.**, 2005, 22, 97-104.

44. SHELTON GD., LIU LA., GUO LT., SMITH GK., CHRISTIANSEN JS., THOMAS WB., SMITH MO.,

Beretta et al.; **Immunohistochemical and Morphometric Evaluation of Gastrocnemius Muscle and Myotendinous Junction of Golden Retriever Dogs with Muscular Dystrophy**. Braz J Vet Pathol, 2014, 7(2), 70 - 81

81

KLINE KL., MARCH PA., FLEGEL T., ENGVALL E. Muscular dystrophy in female dogs. **J. Vet. Intern. Med.**, 2001, 15, 204-44.

45. SILVA JDM., COSTA KS., CRUZ CM. Duchenne Muscular Dystrophy: A kinesiotherapeutic focus (Distrofia muscular de Duchenne: um enfoque cinesioterapêutico). **Lato & Sensu**, 2003, 4, 3-5.

46. SPENCE MJ., WALSH CM., DORSHKIND KA., RODRIGUEZ EM., TIDBALL JG. Myonuclear apoptosis in dystrophic mdx muscle occurs by perforin-mediated cytotoxicity. **J. Clin. Invest.**, 1997, 99, 2745-51.

47. SPENCER MJ., TIDBALL JG. Do immune cells promote the pathology of dystrophin-deficient myopathies? **Neuromuscul. Disord.**, 2001, 11, 556-64.

48. STEVENS A., LOWE J. Sistema nervoso e muscular STEVENS A., LOWE J. Eds. **Patologia**. 2.ed. Manole: São Paulo, 1998, 398-437.

49. TIDBALL JG., WELLING-HENRICKS M. Damage and inflammation in muscular dystrophy: potential implications and relationships with autoimmune myositis. **Curr. Opin. Rheumatol.**, 2005, 17, 703-13.

50. UTZ U., MCFARLAND HF. The role of T cells in multiple sclerosis: implications for therapies targeting the T cell receptor. **J. Neuropathol. Exp. Neurol.**, 1994, 53, 351-8.

51. VAITTINEN S., LUKKA R., SAHLGREN C., HURME T., RANTANEN J., LENDAHL U., ERIKSSON JE., KALIMO H. The expression of intermediate filament protein nestin as related to vimentin and desmin in regenerating skeletal muscle. **J. Neuropathol. Exp. Neurol.**, 2001, 60, 588-97.

52. VALENTINE BA., COOPER BJ., CUMMINGS JF., DE LAHUNTA A. Canine X-linked muscular dystrophy: morphologic lesions. **J. Neurol. Sci.**, 1990, 97, 1-23.

53. VALENTINE BA., CUMMINGS JF., GALLAGHER EA. Development of Duchenne-type cardiomyopathy: Morphologic studies in canine model. **Am. J. Pathol.**, 1989, 135, 671-8.

54. WELSER J., ROONEY JE., COHEN NC., BURKIN DJ. Myotendinous Junction defects and reduced force transmission in mice that lack α7 integrin and utrophin. **Am. J. Pathol.**, 2009, 175, 1545-54.